Prepared for Proceedings of the 23 Annual M.I.T. Conference on Physical Electronics, Cambridge, Mass., March 20-22, 1963

CESIUM DIODE OPERATION IN THREE MODES

Roland Breitwieser

Lewis Research Center
National Aeronautics and Space Administration
Cleveland, Ohio

18p

N65-88655

E-2141

Introduction

The ever-present problem of interpreting operational characteristics of a practical device in terms of past fundamental experiments and analytic treatments appears again in the case of a cesium vapor filled thermionic converter. Some of the experimental difficulties encountered previously in the analysis of voltage-current relations in thermionic converters have been partially circumvented by the introduction of several refinements in the construction of a converter. The primary refinements are the use of a planar diode configuration, an emitter that has an oriented crystal structure, an emitter heater designed for careful control of surface temperature, close fitting guards on the emitter and collector, and variable interelectrode spacing.

This paper presents results of tests conducted in this controlled cesium vapor filled planar diode, which attempt to explore the modes of operation, to measure the work function of tungsten in a cesium atmosphere, and to observe changes in emitter work function associated with a past history of operation at high retarding voltages.

Apparatus and Procedure

The basic features of the converter are shown in figure 1. The thermionic converter is in the form of a planar diode with a demountable emitter and collector. The 1.5-centimeter-diameter, 2.0-centimeter-long emitter structure was formed from tungsten oriented to expose the 110 (Miller index) plane. Most of the surface was a single crystal; however, a few subcrystals existed. The maximum misorientation from the 110 plane was $1\frac{1}{2}^{\circ}$.

The emitter was heated by electron bombardment. The bombardment heater incorporated a deflector that shaped the energy density of the beam to provide a uniform emitter temperature (about $\pm 10^{\circ}$ K) and also prevented most of the filament radiation from entering the field of view of the optical pyrometer.

The emitter guard was flush with the emitter surface. The radial clearance was about 3 mils at operating temperatures. The guard was cooled by conduction. Electrical isolation was provided by alumina insulators.

The collector and support was formed from polycrystalline tungsten. The collector was cooled by gaseous helium. Three equally spaced differential-type micrometer screws on the collector support flange were used to adjust

spacing. "Zero" spacing was established at each operating temperature by lightly touching the three edges in line with the screws. The minimum spacing available was estimated to be 3 to 11 microns.

The collector guard radial clearance was about 3 mils; the guard position was fixed. The guard was recessed about 5 mils behind the collector surface at zero spacing, was cooled by conduction, and was insulated by alumina spacers.

The diode was mounted in a helium-filled oven. Helium jets were used to control the temperatures of the cesium reservoir, the insulator, the guards, the collector, and the diode structure.

The emitter temperature was determined by an optical pyrometer, which viewed the back surface of the emitter through a shuttered window and prism. The problem of spurious radiation from the electron bombardment-heater filament encountered in back surface measurements was avoided by the use of the aforementioned filament-deflector design.

The emitter surface temperature and temperature profile were established in terms of back surface temperature by calibration in a dummy diode structure, which provided for a simultaneous view of the front and the back surfaces. The back surface sighting technique permitted emitter temperature control within $\pm 1^{\circ}$ K during a series of runs (at low current density). Absolute temperatures were determined within the bounds of the usual well-calibrated system.

All internal surfaces other than the emitter and the guarded emitter structure were at temperatures at which only trivial electron emission should occur.

The cesium boiler temperature was measured by thermocouples and was controlled automatically to maintain a prescribed temperature at $\pm 0.10^{\circ}$ K.

The diode bias voltage was provided by a power transistor assembly, switching techniques, and rheostats. The voltage range available was from -90 to +18 volts. An automatic variation in voltage in the form of a 12-volt amplitude triangular wave was available as a single or a continuous sweep. Sweep frequencies from 1/10 to 1000 cycles per second were available. Manual variations in voltage were usually used at low currents. Automatic control was used at high currents.

Separate bias voltages were available to both emitter and collector guards. The emitter guard was allowed to float in the tests reported herein. The collector guard was set at the collector potential for all ion current measurements. Two electron current measurements were usually made, one with the collector guard at the collector potential and one with the collector guard floating.

Data were recorded by the use of differential amplifiers, digital voltmeters, X-Y recorders ($1\frac{1}{2}$-sec writing speed) and oscilloscopes (10 Mc response). Microampere to 100 ampere (plus) current measurements were available.

Discussion

The experimental data under consideration are primarily based on two cesium reservoir temperatures, 469.8°±0.1° K and 499.8°±0.1° K. These temperatures correspond to 6.6×10^{-2} and 0.2 Torr, respectively.

The pressures and spacings place most of the data in the regions of non-collisional behavior up to the case of five mean free paths for electron-neutral collisions (based on a collision cross section σ of 4×10^{-14} cm^2). The primary variable treated is emitter temperature. The temperature range covered is 1350° to 1900° K.

A convenient method of cataloging the conditions is in terms of the ratio of ion to electron emission from the emitter (ref. 1). If the a priori assumption is made that the work functions of cesium-covered tungsten given in reference 1 (based on Houston's experiments, ref. 2) describe the emitter work function and that the Saha-Langmuir equation (ref. 3) roughly describes ion production, the condition of neutral emission can be established. The corresponding emitter temperatures are about 1480° K at a cesium temperature of 469.8° K and about 1555° K at a cesium temperature of 499.8° K. Excess electron emission exists at temperatures less than the "neutral" temperature and excess ion emission at the higher temperature range. The numerical values for the ratio of ion to electron concentration at zero field emission can also be estimated at other temperatures from the use of the Saha-Langmuir equation. Reference 4, a companion paper based on the same 469.8° K cesium temperature data treated herein, indicates that the Saha-Langmuir equation is a reasonable approximation since ion currents are only underestimated by a factor of two to three over much of the range of interest. Larger variations exist in the extreme excess-electron region and in the excess-ion region. The departure in the excess-ion region is largely the ion space charge effect.

Since the Saha-Langmuir equation approximates the ratio of ion to electron emission, it is used to catalog the various results. The actual form used is

$$\frac{\nu_+}{\nu_e} = \frac{\nu_a q \; 120.1 \; T^2}{2J_s^2 \frac{V_i}{V}}$$

and

$$\frac{n_+}{n_e} = \frac{492 \; \nu_+}{\nu_e}$$

At a constant cesium reservoir temperature the following relation can be used:

$$\frac{n_+}{n_e} = \frac{K}{e^{1000/T}} \frac{T^2}{J_s}$$

where ν is flux rate per square centimeter, n is particle concentration, q is unit charge, J_s is saturation current density, T is emitter tempera-

ture in ^{o}K, V_i is ionization potential in electron volts, $\overline{V}$ is electron volt equivalence of temperature, and K is a constant, and the subscripts a refer to atoms, +, to ions, and e, to electrons.

At the conditions when the Saha-Langmuir relation is not an adequate index of ion currents the concentration ratio based on measured ion current is also included in the description of the results. Small inconsistencies may exist in the n_+/n_e ratio given in reference 4 and those calculated from the above form of the Saha-Langmuir equation. This is due to the use of measured saturation current density in the preceding equation.

Space Charge Mode

The first mode treated relates to current-voltage characteristics subject to space-charge effects. Langmuir space-charge theory (ref. 5) could be expected to describe current-voltage characteristics where the charge concentration is predominantly electron or ion. The close spacing (3 to 11 μ) and guarded structure permit a reasonable test of the space-charge theory. Close spacing permits the determination of saturation currents, which, in turn, establishes the emitter work function. The accuracy of current flow measurements in the retarding region is improved by the emitter and collector guards and thus collector work functions are accurately determined. No arbitrary parameters are used in the space-charge analysis since the difference in surface potentials, spacings, saturation currents, and emitter temperature are all measured or directly calculated quantities. The procedures used in actual solution are similar to those outlined in references 6 to 8.

A detailed comparison of the current calculated by the Langmuir space-charge theory to measured values was made at two emitter temperatures, two spacings, and a cesium reservoir temperature of 469.8° K.

The conditions examined are in the excess-electron region. The ratios of ion to electron concentration are as follows:

Emitter temperature, ^{o}K	n_+/n_e	
	Saha-Langmuir	Measured
1352	0.007	0.09
1372	.018	.15

(See ref. 4 for explanation of the discrepancy in n_+/n_e.)

The comparison of measured current to the current calculated by space-charge relations when electron emission only is assumed is as follows:

Difference in surface barrier potential, qV/kT, V/$\overline{V}$ (dimensionless volts)	Emitter temperature, °K			
	1352		1372	
	Spacing, μ			
	[a]8	57	8	57
	Measured current/calculated[b] current			
-5	1.0	1.0	1.0	1.0
-3	1.0	1.0	1.0	1.0
-1	.9	1.0	.90	1.0
0	.60	1.0	.70	1.15
1	.60	1.0	.70	1.1
3	.60	.90	.80	1.0
5	1.0	.75	.95	.85
10		[c].60	1.0	[c].65
15		.60		.8
20		.75		.9

[a]The best estimate is 3 to 11 μ; 8 μ is an arbitrary selection.

[b]All values rounded to nearest 0.05 value.

[c]Saturation current exists on basis of Langmuir space-charge theory.

The agreement between space-charge theory and the experimental 8-micron data is fair. Agreement also exists for the 57-micron spacing up to a positive surface potential difference of 3 (qV/kT). Beyond this point, however, the measured current is significantly lower than the calculated value. In general, the currents measured at the larger spacings do not approach saturated current values (determined by close-spacing data) as quickly as the space-charge theory would predict. The existence of ion emission would be expected to permit saturation to occur at lower values of applied potentials (ref. 9) instead of the observed effect.

The results indicate that the noncollisional Langmuir space-charge theory gives fair quantitative agreement at the closest spacing. The agreement deteriorates as spacings are increased and the condition of collisional activity is approached. (The mean free path for electron-neutral collisions is about 310 μ at the conditions cited in the preceding table.)

The space-charge analyses that treat both ion and electron emission are complex. Special cases have been treated in references such as 9 to 12. It is not the objective of this paper to attempt to make detailed comparisons of experimental results with these analyses but merely to indicate a few general trends. Figures 2 to 4 present current-voltage characteristics in order of increasing ion/electron concentration. The various conditions of operation are indicated in the figures.

Current is reduced as spacing is increased in general accord with space-charge analysis (e.g., fig. 2); but as in the case of 1352° and 1372° K

emitter temperatures the larger spacing exhibit currents lower than that predicted by simple space-charge theory. The monatomic solutions of the combined electron emission (e.g., ref. 9) predict smaller space-charge barriers than the single-charge case; thus even greater departures of theory from experiment are indicated. Reference 9 also indicates that the space-charge barrier should be removed at an n_+/n_e ratio of 0.5. Experimental results show that at n_+/n_e ratios greater than 4.2 space-charge behavior still persists (fig. 3). The set of data obtained at a cesium reservoir temperature of 469.8° K requires an n_+/n_e ratio of 16 in order to remove the space-charge barrier. An example of current-voltage characteristics at a high ratio of n_+/n_e is given in figure 4.

Ignited and Arc Modes

In addition to space-charge modes, ignited and arc modes of operation are also observed. The definitions are somewhat arbitrary and are based on saturation currents measured at the smallest spacings. The ignited mode is characterized by a discontinuity in current as voltage is increased, after which saturation current is reestablished. A hysteresis is noted in that, after ignition occurs, the voltage may be decreased while saturation current is maintained. After still further reductions in voltage, the current returns to the value that existed prior to ignition. An example of ignited mode is shown in figure 2 (227-μ spacing).

The arc and the ignited modes are similar since in both a discontinuity in current occurs with an increase in applied voltage. The hysteresis effect is also observed. The uniqueness of the arc mode is that the current increases beyond saturation values with continued increases in applied voltages. An example of the arc mode is the 3 to 11 micron spacing curve in figure 5.

It is difficult to establish whether the arc mode exhibits a new upper limit in current density. Severe electron cooling of the emitter (and heating of the collector) often coupled with high-frequency oscillations confuse the issue. Momentary values of current density over 100 amperes per square centimeter have been observed at a cesium reservoir temperature of 500° K and emitter temperatures in the range of 1500° to 1600° K.

The ignited mode is observed at spacings of 227 microns at emitter temperatures of 1420° K and cesium temperatures of 469.8° K (fig. 2). No evidence of ignition exists at higher emitter temperatures (figs. 3 and 4) even though space-charge behavior is evident. The ignited mode exists at emitter temperatures of 1498°, 1536°, and 1568° K when the cesium reservoir temperature is 499.8° K (figs. 5 to 7). Again there is no evidence of ignition at spacings of 113 microns or less. The mean free path for electron-neutral collisions at conditions of figure 2 is 320 microns; for figures 5 to 7 it is about 115 microns. The mean free path based on charge exchange cross sections of ion-neutrals is about one-sixth of that based on the electron-neutral collisions. (Note that this approximate relation is based on values of cross sections from ref. 13.)

The requirement of nearly one mean free path and applied voltages near the ionization potential in figures 2 and 5 suggests that volume ionization

is coincident with ignition. The ignition voltages substantially less than the ionization potential of figures 6 and 7 can be argued as being related to stepwise ionization processes.

In contrast, the oscillations present before ignition (figs. 5 to 7) are somewhat consistent with the instabilities predicted by the space-charge theories of references 10 to 12. This, coupled with a high probability of ion-neutral collisions, could be used to establish that the ignited mode is not due to volume ionization and ignition but is merely a consequence of ion trapping. Sufficient surface ions are produced to satisfy an ion-trapping model since the ion-electron ratios shown underestimate the ion production rates by a factor of 2 or more (refer to space-charge discussion or ref. 4).

The arc mode is clearly evident in figures 5 to 7 at all spacings. Applied potentials near the ionization potential of cesium induced the arc mode at the 499.8° K cesium reservoir condition for the emitter temperature illustrated. At emitter temperatures (not shown) of 1800° K and above the tendency to arc was suppressed.

The results shown in figure 7 illustrate a clear distinction between arc mode and the ignited mode. An anomaly exists since the current jumps to the values observed at the 113-micron spacing after ignition rather than going directly to saturation values.

Ignition occurred at slightly less than +1 volt for the 227- and 340-micron spacings. The current jumped to the level of the 133-micron spacing after ignition. The currents for the three spacings were essentially the same up to the point of a second ignition. After the second ignition a common arc mode current was established for all spacings.

The arc mode seems clearly associated with high ion production rates and appears analogous to arcs experienced in other gaseous discharges. The ignited mode is less well defined.

Work Function Measurements

Space-charge analyses of close-spacing data supported by reestablishment of saturation currents after most ignitions indicate that saturation currents can be measured accurately in a variable spacing, guarded diode. Estimates of the effective work function follow directly from saturation currents through the use of the Richardson-Dushman emission equation. A comparison of values based on current density of the diode to those estimated by Nottingham (ref. 1) from Houston's emission probe measurements (ref. 2) is shown in figure 8. The work functions estimated in reference 1 are shown in the form of a chart in the companion paper (ref. 4). The diode data shown in figure 8 encompass a range of values of emitter temperature of 1350° to 1900° K and cesium pressures of 7×10^{-2} to 1.3 Torr. The agreement is self-evident.

Cathode Effect

It was noted that a consistent increase in work function occurred after operation at a high retarding voltage for the purpose of obtaining ion current data. These data are indicated by the tailed data points in figure 8.

Typical current-voltage characteristics associated with these data are illustrated in figure 9. The change in work function with operating conditions is termed the "cathode effect" because of a somewhat analogous "anode effect" observed by Nottingham (ref. 14).

An increase in emitter work function of approximately 0.05 electron volt was observed after operation at -80 volts and an emitter temperature of 1502° K for a period of 30 seconds. A similar change was noted at -50 volts, 1648° K, and a period of 60 seconds. The normal emission could be reestablished if the diode was maintained at zero applied potential. The reactivation period appeared to exhibit an inverse exponential relation, that is, reactivation time was rapidly decreased with increases in temperature. It was also noted that the change in work function exhibited a threshold behavior, which was dependent on both field strength and retarding voltage.

The change in work function was not noted at temperatures greater than 1760° K presumably because of the rapid reactivation times.

The cathode effect casts some doubt on the nature of the emitter surface. Although efforts were made to establish diode cleanliness and emitter definition through the use of an oriented tungsten crystal, the change in work function indicates that the substrate for cesium was probably something other than 110 tungsten.

Concluding Remarks

The results indicate the existence of three discrete modes of operation, the space-charge mode, the ignited mode, and the arc mode. The ignited mode may not be a true ignition in the sense of being related to volume ionization. Observation of the various modes of operation coupled with operation at a close spacing permits the determination of emitter work functions. The work functions measured in this tungsten-cesium thermionic converter agree with values determined by emission-probe measurements. A change in emitter work function dependent on field and magnitude of retarding voltage was noted and conditions of occurrence approximately established.

References

1. Nottingham, W. B.: Sheath and Plasma Theory of an Isothermal Diode. Rep. 4-62, Thermo Electron Eng. Corp. (1962).

2. Houston, J. M.: Thermionic Emission of Refractory Metals in Cesium Vapors. Bull. Am. Phys. Soc. 6, Ser. II, 358 (1961).

3. Kingdon, K. H., and Langmuir, I.: Proc. Roy. Soc. London A107, 61 (1925).

4. Nottingham, W. B.: Cesium Ion Production in a Strong Ion Accelerating Field. Twenty-Third Ann. Conf. on Phys. Electronics, M.I.T. (1963).

5. Langmuir, I.: Phys. Rev. 21, 419 (1923).

6. Ferris, W. R.: Some Characteristics of Diodes with Oxide-Coated Cathodes. RCA Review 10, 134 (1949).

7. Nottingham, W. B.: Thermionic Emission. Rep. 321, Res. Lab. of Electronics, M.I.T. (1956).

8. Webster, H. F.: Calculation of the Performance of a High-Vacuum Thermionic Energy Converter. J. Appl. Phys. 30, 4, 488 (1959).

9. Hansen, L. K., and Warner, C., III: Emission Requirements for Removal of Space Charge Barriers. Second Annual Tech. Summary Rep. for Basic Res. in Thermionic Energy Conversion. AI 7979 (1962).

10. Aurer, P. L.: J. Appl. Phys. 31, 2096 (1960).

11. Hernquist, K. G.: RCA Rev. XXII, 7 (1961).

12. McIntyre, R. G.: J. Appl. Phys. 33, 2485 (1962).

13. Sheldon, J. W.: Mobilities of the Alkali Metal Ions in Their Own Vapor. J. Appl. Phys. 34, 2, 44 (1963).

14. Nottingham, W. B.: Phys. Rev. 49, 78 (1935).

THERMIONIC CONVERTER

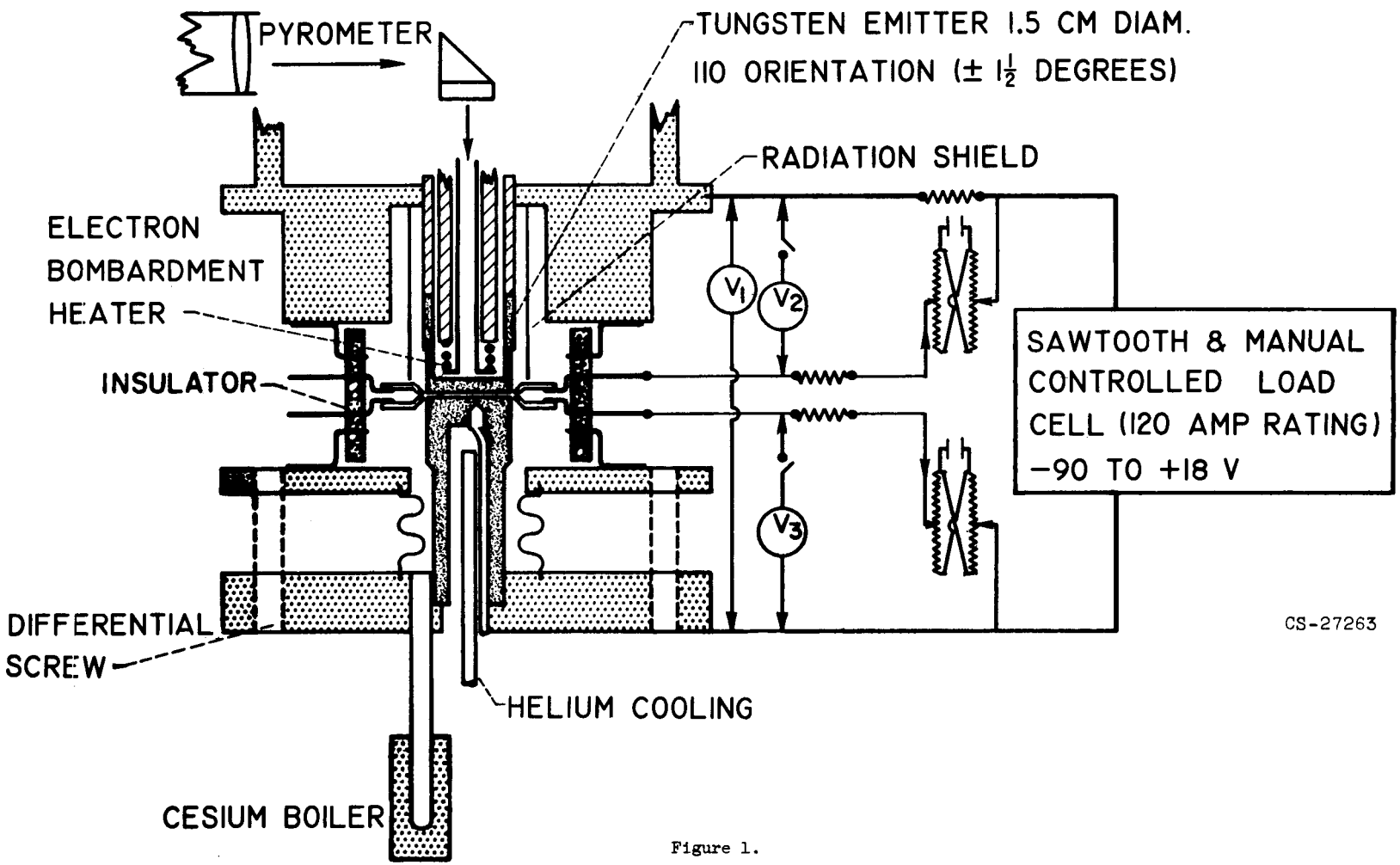

Figure 1.

CURRENT–VOLTAGE CHARACTERISTICS
EXCESS ELECTRON REGION, $\frac{n_+}{n_e}$ = 0.066 (APPROX.)

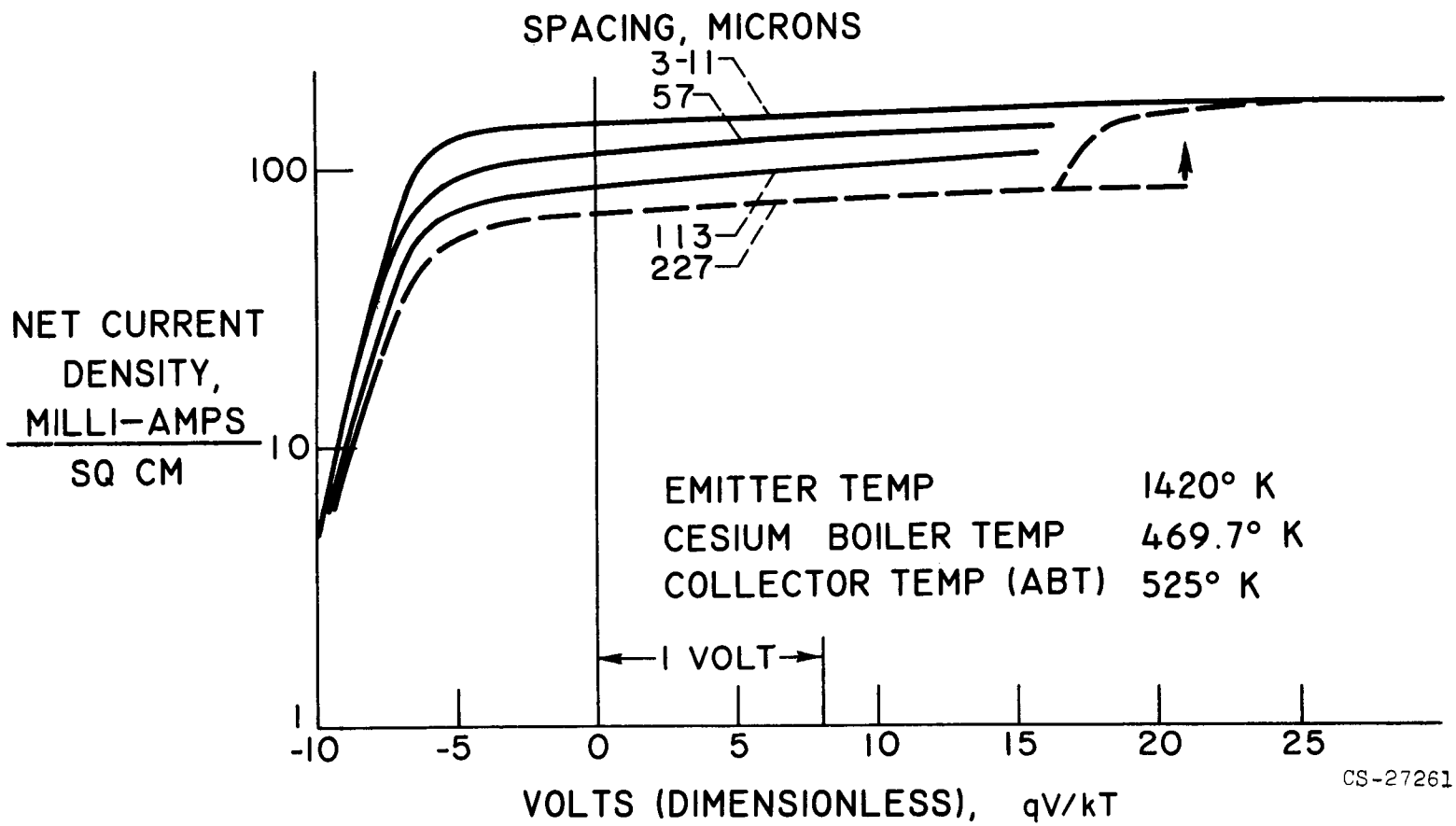

Figure 2.

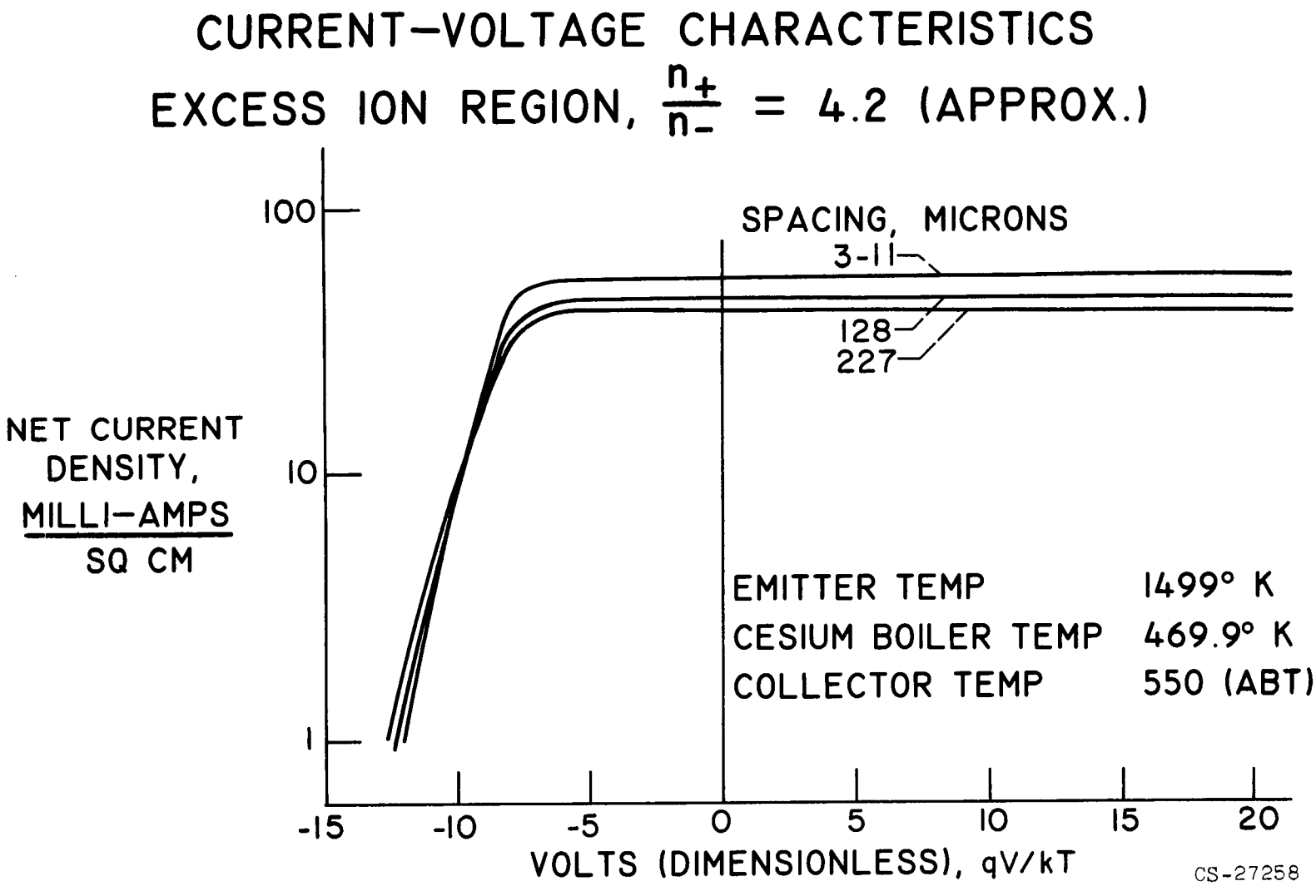
CURRENT–VOLTAGE CHARACTERISTICS
EXCESS ION REGION, $\frac{n_+}{n_-}$ = 4.2 (APPROX.)
NET CURRENT DENSITY, MILLI–AMPS / SQ CM
100
10
1
SPACING, MICRONS
3-11
128
227
EMITTER TEMP 1499° K
CESIUM BOILER TEMP 469.9° K
COLLECTOR TEMP 550 (ABT)
-15
-10
-5
0
5
10
15
20
VOLTS (DIMENSIONLESS), qV/kT
CS-27258

Figure 3.

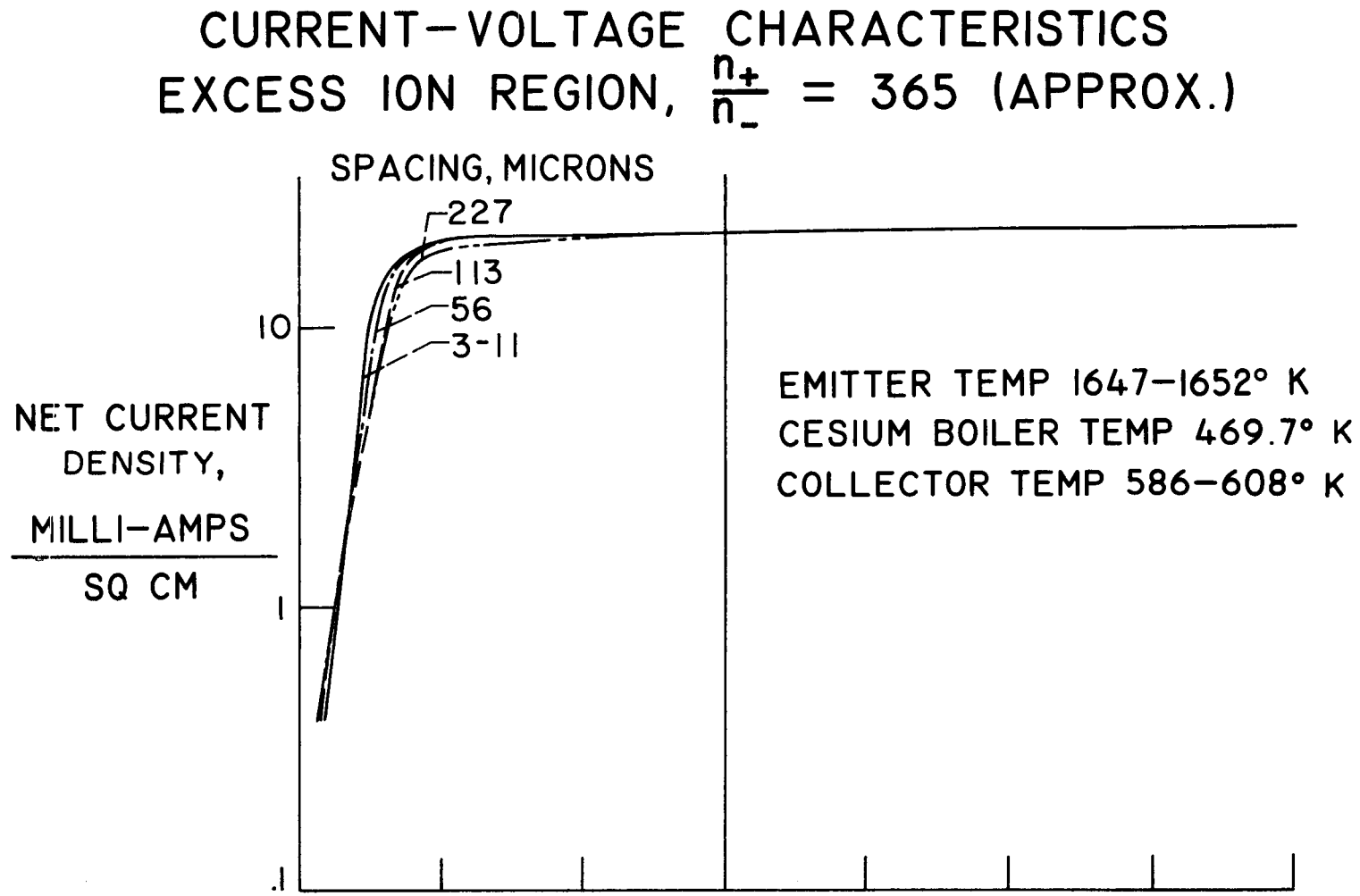
CURRENT–VOLTAGE CHARACTERISTICS
EXCESS ION REGION, $\frac{n_+}{n_-}$ = 365 (APPROX.)
SPACING, MICRONS
227
113
56
3-11
10
1
.1
NET CURRENT DENSITY, MILLI–AMPS / SQ CM
EMITTER TEMP 1647–1652° K
CESIUM BOILER TEMP 469.7° K
COLLECTOR TEMP 586–608° K
-15
-10
-5
0
5
10
15
20
VOLTS (DIMENSIONLESS), qV/kT
CS-27257

Figure 4.

CURRENT–VOLTAGE CHARACTERISTICS EXCESS ELECTRON REGION, $\frac{n_+}{n_-} = 0.18$

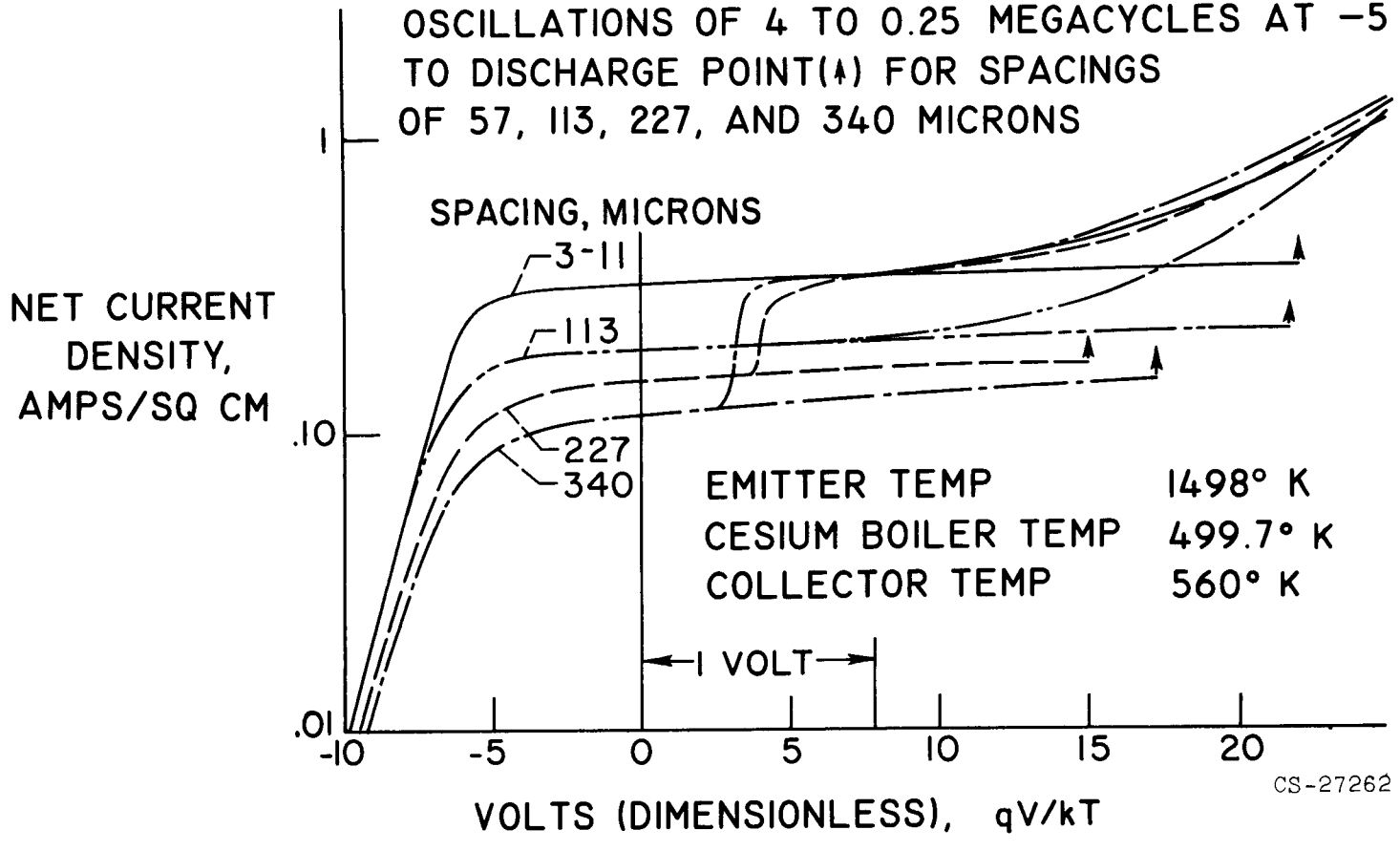

Figure 5.

CURRENT–VOLTAGE CHARACTERISTICS IN SLIGHTLY EXCESS ELECTRON REGION $\frac{n_+}{n_e}$ = 0.4 (APPROX.)

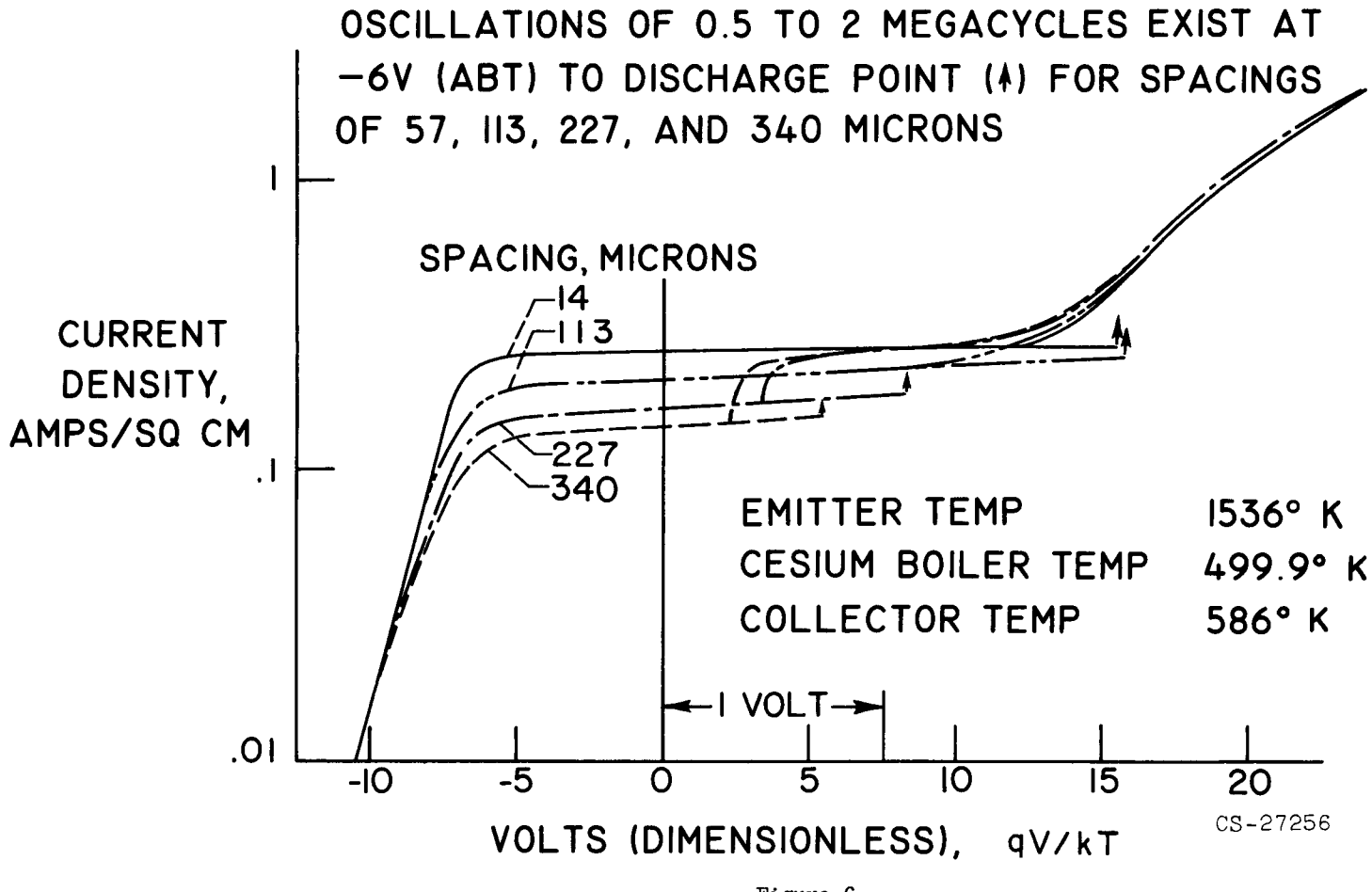

Figure 6.

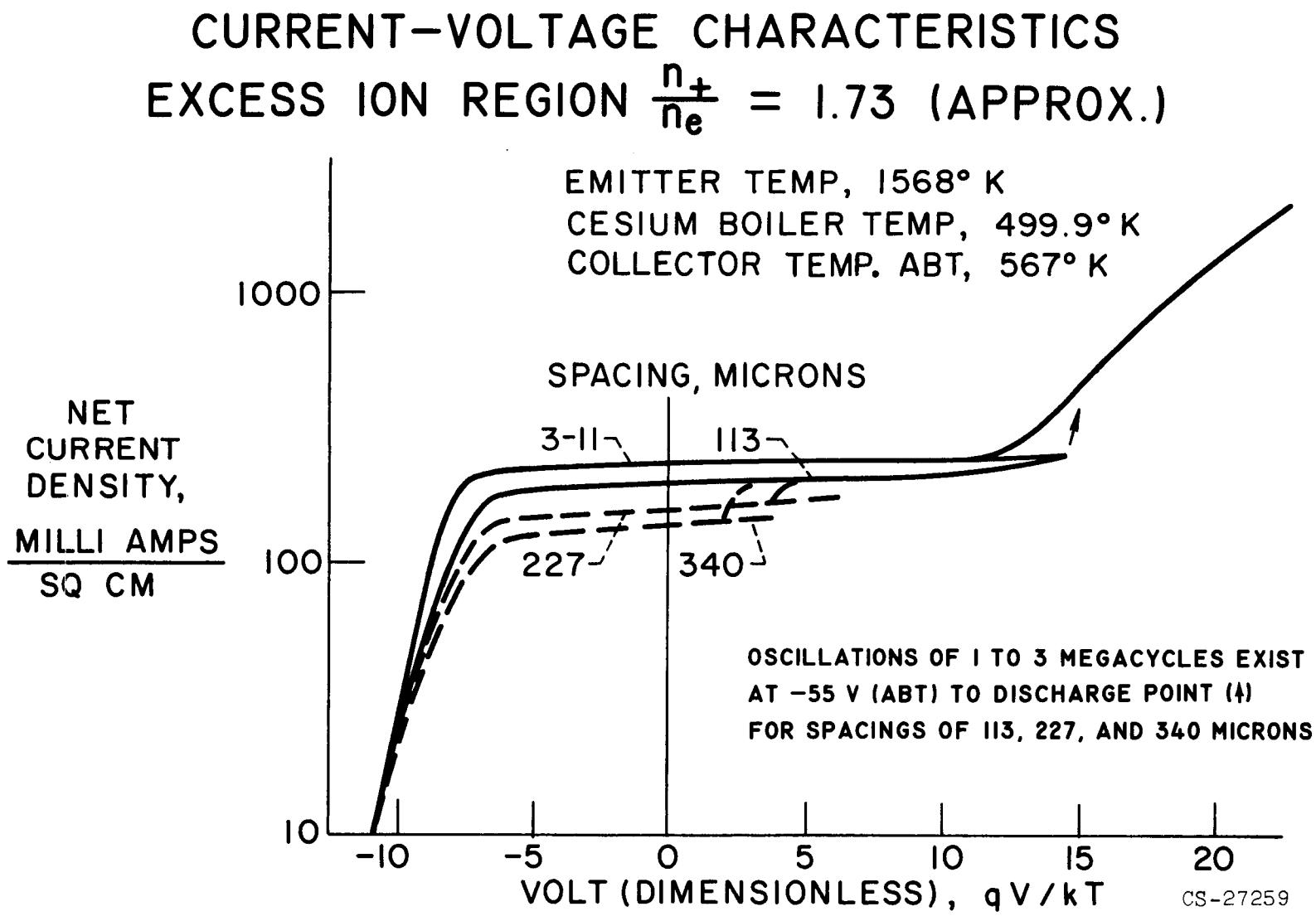
CURRENT–VOLTAGE CHARACTERISTICS
EXCESS ION REGION $\frac{n_+}{n_e}$ = 1.73 (APPROX.)
EMITTER TEMP, 1568° K
CESIUM BOILER TEMP, 499.9° K
COLLECTOR TEMP. ABT, 567° K
SPACING, MICRONS
3-11
113
227
340
NET CURRENT DENSITY, MILLI AMPS / SQ CM
1000
100
10
OSCILLATIONS OF 1 TO 3 MEGACYCLES EXIST
AT −55 V (ABT) TO DISCHARGE POINT (4)
FOR SPACINGS OF 113, 227, AND 340 MICRONS
−10
−5
0
5
10
15
20
VOLT (DIMENSIONLESS), qV/kT
CS-27259

Figure 7.

COMPARISON OF WORK FUNCTIONS BASED ON CURRENT DENSITY TO VALUES FROM REF. I

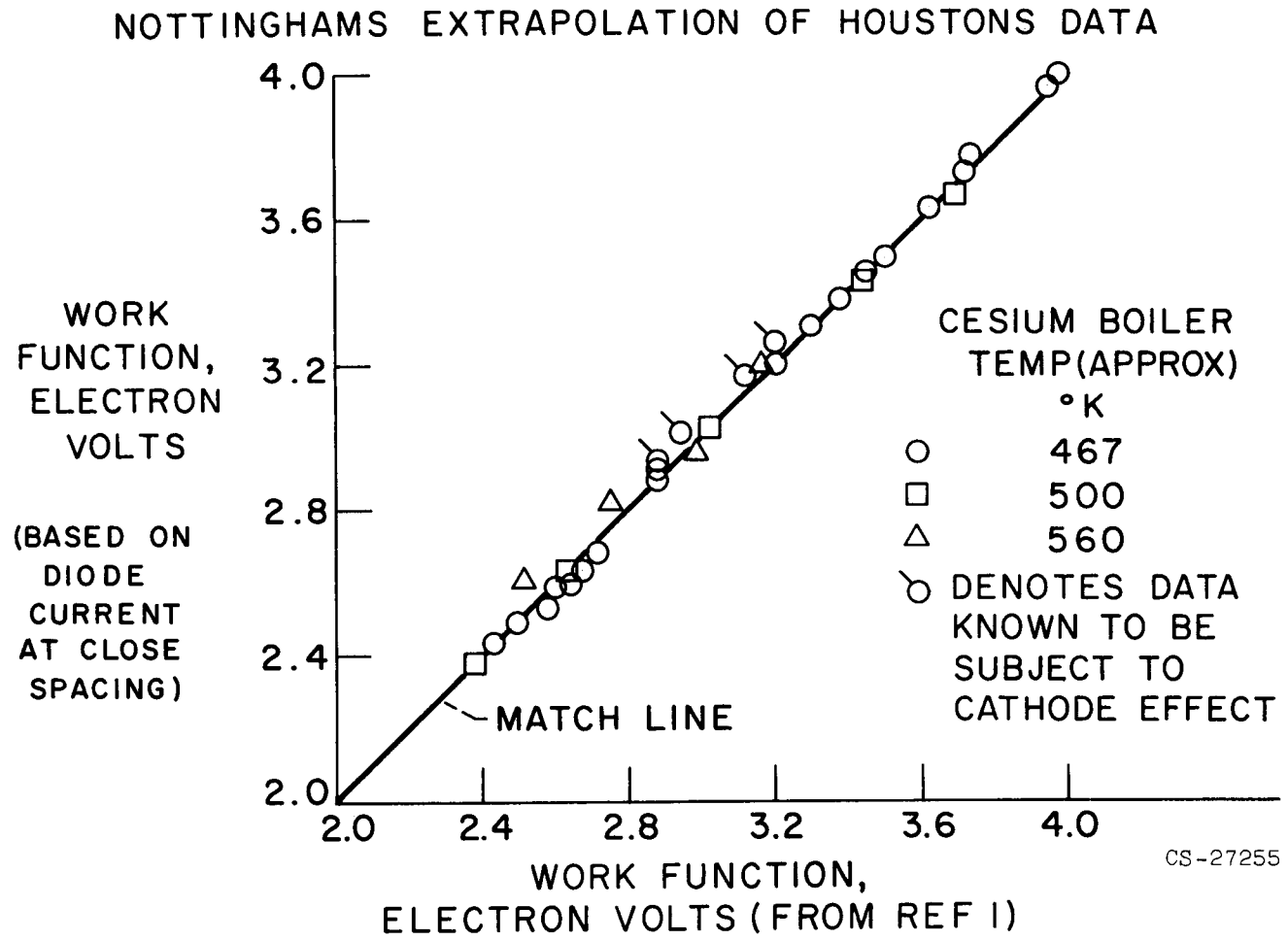

Figure 8.

CATHODE EFFECT

CHANGE IN EMITTER WORK FUNCTION CAUSED BY A RETARDING FIELD

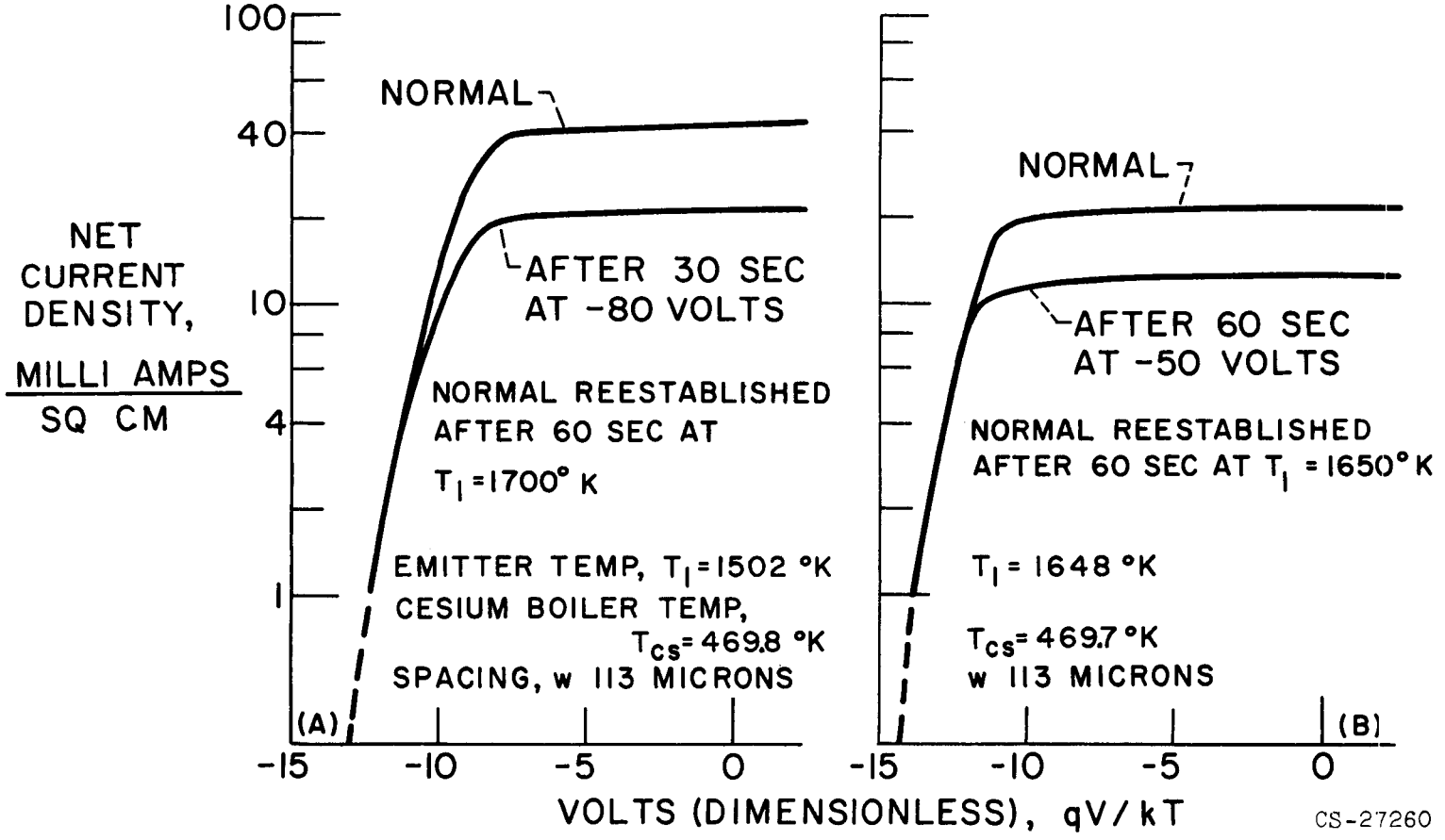

Figure 9.